doi:10.3788/gzxb20174609.0901003

非对称空间外差干涉仪相位探测和漂移校正

沈静[1,2,3],熊伟[1,2,3],施海亮[1,3],罗海燕[1,3],方雪静[1,2,3],
李志伟[1,3],胡广骁[1,2,3],徐标[1,2,3]

(1 中科院合肥物质科学研究院 安徽光学精密机械研究所,合肥 230031)
(2 中国科学技术大学,合肥 230026)
(3 中科院光学表征与定标重点实验室,合肥 230031)

摘 要:针对多普勒非对称空间外差干涉技术,提出一种目标信号相位自校正的方法.首先通过连续采样单色光的干涉图跟踪绝对相位漂移;然后分段线性拟合不同风速下的干涉相位,通过计算两条拟合曲线距离去除相位漂移.搭建风速模拟实验平台,获得采样干涉图,并对相位误差进行校正.结果表明,在60.37 m/s 的模拟风速下,相位漂移误差达到 30.78 m/s,通过相位校正风速反演误差降低至 3.51 m/s,风速精度得到较大改善.最终通过几组不同风速下的反演值得到了平均 2.97 m/s 的风速测量精度.

关键词:傅里叶变换;光谱分析;干涉图测量;相位频移;风速

中图分类号:O433.4 **文献标识码**:A **文章编号**:1004-4213(2017)09-0901003-7

Phase Detection and Drift Correction for Doppler Asymmetric Spatial Heterodyne Interferometer

SHEN Jing[1,2,3], XIONG Wei[1,2,3], SHI Hai-liang[1,3], LUO Hai-yan[1,3],
FANG Xue-jing[1,2,3], LI Zhi-wei[1,3], HU Guang-xiao[1,2,3], XU Biao[1,2,3]

(1 *Anhui Institute of Optics and Fine Mechanics, Hefei Institutes of Physical Science, Chinese Academy of Sciences, Hefei* 230031, *China*)
(2 *University of Science and Technology of China, Hefei* 230026, *China*)
(3 *Key laboratory of Optical Calibration and Characterization of Chinese Academy of Sciences, Hefei* 230031, *China*)

Abstract: A target signal phase self-correction method was proposed for Doppler asymmetric spatial heterodyne technique. First by sampling the interferogram frames of monochromatic light under different wind speed continuously, the phase drift was recorded. Then by fitting the phase curves at different speed and calculating the distance between two fitting lines, the phase drift was eliminated. The wind detection system was established in the laboratory to obtain the sampling interferogram and correct the phase error. The result shows that the error is up to 30.78 m/s at the wind speed of 60.37 m/s, and there is a great improvement after phase drift correction with a speed error of 3.51 m/s. Several groups of experiment under different wind speed were conducted and the wind speed was retrieved with a precision of 2.97 m/s finally.

Key words: Fourier transform; Spectrum analysis; Interferogram measurements; Phase shift; Wind speed

OCIS Codes: 010.0280; 010.1290; 300.6300; 300.6320; 300.2140; 280.4991

Foundation item: xx-5 Satellite Data Simulation Project(No.50-Y20A38-0509-15/16)

First author: SHEN Jing(1988—), female, Ph.D degree candidate, mainly focus on the wind speed detection in the upper atmosphere. Email:xingyang_jing@163.com

Superisor(Corresponding author): XIONG Wei(1975—), male, Ph.D degree, senior scientist, mainly focus on the remote sensing on high spectrum. Email:frank@aiofm.ac.cn

Received: Mar.14, 2017; **Accepted**: May.17, 2017

0 Introduction

Passive wind detection has been applied in the upper atmosphere for decades[1]. Beginning with Fabry-Perot interferometer, wind speed can be calculated from the shift of a single fringe[2-4]. Fabry-Perot interferometer has high sensitivity, but stringent optical flatness and low etendue[2]. With the development of field-widened technique, Michelson interferometer was used in the wind detection[5-6]. Wind speed is derived from fringe phase. Despite the large etendue, only four points are sampled using the stepper motor[7-8]. Recent years, Doppler Asymmetric Spatial Heterodyne (DASH) technique is proposed to measure the wind speed[9]. Without moving parts, DASH interferometer can measure hundreds of points in a large Optical Path Difference (OPD) interval. It has high etendue and can observe multiple emission lines simultaneously[10-13]. The typical ground-based instrument (Redline DASH Demonstration Instrument, REDDI) has successfully detected the airglow in the upper atmosphere [10]. After that a space-based instrument Michelson Interferometer for Global High-resolution Thermospheric Imaging (MIGHTI) is being developed[14].

Since DASH interferometer heterodynes the spatial fringe frequency around Littrow wavenumber of the gratings, interference phase drifts obviously due to the change of Littrow wavenumber. To eliminate the slow drift of the interference system, calibration lamp is used for simultaneous phase tracking[11-12]. Nevertheless, it has wavelength dependence that can be found in the reference[12]. The calibration wavelength must be chosen very closing to the target emission line in order to track the drift effectively. For the near-infrared airglow, it is difficult to find appropriate calibration source. A wavelength difference (the difference of the target line and the calibration line) of 6.4 nm can lead to the phase error of 2.62 mad, which leads to a wind retrieval error that can't be ignored.

The innovative idea in this paper is to realize the phase correction by sampling the interferogram continuously without using the calibration light source. Through linearly fitting the phase curve and calculating the distance between zero wind and a given wind speed, the phase drift is eliminated and the wind speed is retrieved.

1 Experimental research

Based on the optical Doppler theory, the relationship between interference phase shift caused by the moving airglow particles and OPD can be written as [3]

$$\delta\phi = 2\pi L\sigma \frac{v}{c} \tag{1}$$

where L is OPD, σ is the wave number, v is the wind speed and c is the light speed. Phase shift is obtained by subtracting the zero wind phase. Using DASH technique, absolute phase is calculated from the ratio of the interference imaginary and real part[9].

The schematic is shown in Fig.1[9]. Airglow in the upper atmosphere enters the beam splitter after collimated by lens 1 (L_1). The parallel light is divided into two beams. The transmitted beam and reflected beam travel to the surfaces of two gratings (G_1 and G_2) and come back to beam splitter to form the fringe pattern. Using imaging lenses (L_2 and L_3) the fringe is zoomed on CCD detector. The difference between DASH and SHS technique is the OPD (L_{opt}) introduced by one arm's offset of Δd.

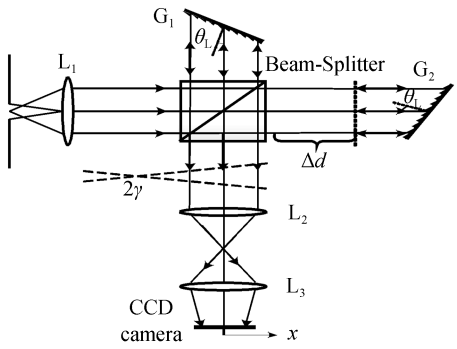

Fig.1 Schematic of a DASH interferometer

$$L_{opt} = 2\Delta d = \frac{1}{2\pi\sigma_D}$$
$$\sigma_D = \sigma_0\sqrt{\frac{kT}{mc^2}} \tag{2}$$

where σ_D is the line width, T is the temperature, m is the mass of the emitter, σ_0 is the wave number of the line center, and k is the Boltzmann constant.

In this article, a DASH interferometer that used to detect the O_2 A-band airglow is developed. The interferometer is designed with double arm structure in order to satisfy the large L_{opt} (L_{opt} = 6.15 cm based on Eq.(2)). It is realized by adding a large spacer between the prism and grating in the long arm.

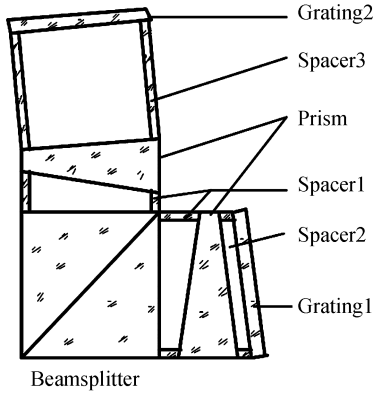

Fig.2 Schematic of the DASH interferometer

The interferometer contains four components: a beam splitter, two field-widened prisms, spacers that made of fused silica and two diffraction gratings which are replicated on fused silica substrate. In the DASH interferometer, the signal is split in two beams. Light beam in the long arm travels to the surfaces of grating via field-widened prism and a long spacer. At the same time light beam in the short arm travels to grating via field-widened prism and a short spacer. They come back to beam splitter and form the fringe pattern. The main parameters are shown in Table 1.

Table 1 Design parameters of DASH interferometer

Parameter		Value
Beam splitter	Size/mm	50×50
Spacer 1	Thickness/mm	10
	Bottom angle/(°)	77.5379
Prism (Silica)	Refraction	1.4539862@766.49 nm
	Thickness/mm	11
	Bottom angle-α_1/ (°)	77.537 9
	Bottom angle-α_2/ (°)	85.369 2
	Apex angle/ (°)	17.092 9
Spacer 2	Thickness/mm	7
Spacer 3	Thickness/mm	62
Grating	Groove density/(gr • mm^{-1})	600
	Littrow angle/ (°)	13.1264
Scaling		0.621

The Potassium Hollow Cathode Lamp (HCL) is chosen for their isolated emission lines in the pass band near the wavelengths emitted by excited oxygen in the upper atmosphere. The filter was designed to provide a 15 nm band FWHM in the region. The data is collected on a CCD camera, which contains a monochromatic 1 024 pixel×1 024 pixel. The 2.2 cm images of the fringe localization plane, which is located near the grating, are focused onto the camera with a commercial lens with × 0.6 magnification.

To validate the wind detection ability in the laboratory, Doppler wheel is designed to produce the wave number shift. The retro-reflecting tape is covered on the disk so that the incidence beam can go back to the system on the same direction (Fig. 3). When the disk is driven by the motor at a rotating speed n, the reflected beam will carry the speed as

$$v = 4\pi n r \cos\alpha \qquad (3)$$

where r is the distance from light beam to the plate center , α is the angle between optical axis and disk. The wave number of the light source will shift as

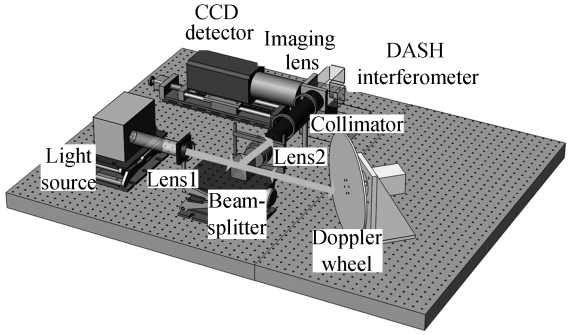

Fig.3 Schematic of the experimental setup

$$\delta\sigma=\sigma_0 \cdot v/c \tag{4}$$

where σ_0 is wave number of light and c is the velocity of light.

Relying on the instruments above, the laboratory system to detect the Doppler shift is established.

The experiment is mainly composed by the pre-shift device and interferometer system. Light from HCL is collimated by lens1. The parallel beam travels through a beam splitter and then reaches the Doppler wheel. Coating with a retro-reflecting tape on the plate, light returns back to the beam splitter along the same direction. The parallel beam is collected by lens 2. After entering the interferometer system and forms the fringe, the interferogram is recorded by the CCD detector.

2 Phase drift correction method

According to Eq.(1), the phase sensitivity of the DASH interferometer is 0.0034 rad at 1 m/s. To detect such small phase change, the light source used in the laboratory must be stable enough. Potassium hollow cathode lamp (HCL) is chosen with the target emission line of 766.49nm. The zero wind interferogram was sampled when the Doppler wheel was still and a shift interferogram was sampled when the Doppler wheel rotated at 3600 RPM (60.37 m/s). The phase shift curve was calculated based on the function in Ref.[9].

It is noted that 20 groups of single measurement at the same wind speed (60.37 m/s) were conducted independently, which is shown in Fig.4 as the phase curves with different colors. Ignoring the obviously distortion at both ends due to the convolution of the window function, the phase shift curves has large uncertainty among different experiments. For example, the phase difference at $L_{opt}=12.29$ cm varies from 0.207 7 to 0.228 5 rad among the twenty measurements, which is corresponding to a speed uncertainty of 6.12 m/s. It is probably comes from the slow drift of the system since the environmental changes during sampling the interferogram.

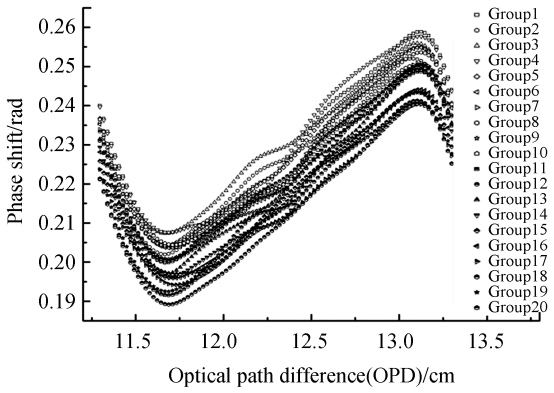

Fig.4 The relationship between OPD and the phase shift

Therefore a method is proposed to eliminate the drift in the absolute phase. The CCD detector is configured as continuous sampling. The interferogram series I_0 under zero wind speed is sampled with the length of N. Then the interferogram series I_v under a given wind speed is sampled with the same length. The absolute phase at L_{opt} was calculated and expressed as

$$\begin{aligned}\phi_0&=[\phi_{01}\ \phi_{02}\ \phi_{03}\cdots\phi_{0(N-1)}\ \phi_{0N}]\\ \phi_v&=[\phi_{v1}\ \phi_{v2}\ \phi_{v3}\cdots\phi_{v(N-1)}\ \phi_{vN}]\end{aligned} \tag{5}$$

where ϕ_0 is the absolute phase at 0m/s and φ_v is the absolute phase at speed of v.

The least square method is used to fit the absolute phase curves (ϕ_0 and ϕ_v) and we can get the linear fitting function as

$$\begin{aligned}y_1&=k_1x+b_1\\ y_2&=k_2x+b_2\end{aligned} \tag{6}$$

where x is the frame number of the sampled interferogram, k_1 and k_2 is the slope of the fitting phase of φ_0 and ϕ_v. It is noted that the slope k_1, k_2 indicates the phase drifts error. In the perfect situation, $k_1=k_2=0$ and the phase shift $\delta\phi=b_1-b_2$. While the system error, random noise and the temperature change of the environment all lead to the phase change. Since I_0 and I_v is sampled continuously, phase drift of k_1 and k_2 has similar trend. Therefore by calculating the distance from the middle point of $y_2(x_m, y_m)$ to y_1, the phase shift can be obtained without phase drift error.

$$\delta\phi=\frac{|k_1x_m-y_m+b_1|}{\sqrt{k_1^2+b_1^2}} \tag{7}$$

where $\delta\phi$ is the phase shift. According to the distance of point to line function, the phase shift can be

calculated in Eq.(7).

3 Result

Based on the method, a group of interferogram was sampled to correct the phase drift and achieve the wind speed with high precision. In the laboratory, the Potassium hollow cathode lamp was started at 10 mA and the CCD detector was cooled to −40℃. The integral time was 0.5 s with a total sampling length of 120. To keep a relative stable environment, the air-condition was closed when the room temperature was 25℃ (outside temperature was 35℃). First, 50 frames of interferogram at 0 m/s were sampled continuously. Then the Doppler wheel was started to a stable rotating speed of 3 600 RPM and 50 frames interferogram at 60.37 m/s were sampled again. It is noted that 10 s was cost to adjust the motor rotating speed during which 20 frames of invalid interferograms were also sampled. With the Fourier Transformation (FT) and Inverse Fourier Transformation (FT^{-1}), the complex interferogram with shift is achieved. Fig.5 shows the real part of the complex interferogram from 50 frame and 71 frame which is corresponding to the zero wind speed and 60.37 m/s wind speed.

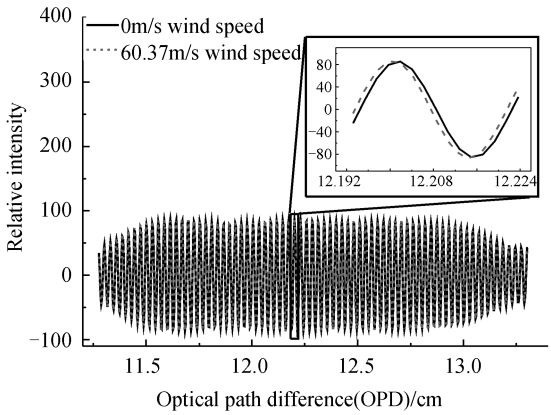

Fig.5 The real part of the complex interferogram

The fringe number of 766.49 nm is 73. It is difficult to distinguish the fringe shift in the full OPD area, as can be seen in Fig.5. Thus a fringe period (in the right top corner) is picked up from 12.195 cm to 12.220 cm to see the fringe shift caused by the Doppler wind speed clearly. Even though the DASH interferometer is designed with large offset, the fringe shift is still small. Therefore the phase shift is small and the system error has a significance influence on the wind retrieving.

Generally, the absolute phase at L_{opt} was used to retrieve the wind speed. Through row average phase value can be obtained from a single interferogram. The phase curve is divided into three parts which is corresponding to the sampling process described in the last paragraph. Despite the adjusting process of the rotate speed from 51 to 70 frames, it is indicated that the absolute phase decreases linearly with the sampling. It is caused by the decreasing of the Littrow wavenumber. By fitting the absolute phase curve using least square method, the function is shown in the left corner of Fig.6. Round symbol line is the phase curve at 60.37 m/s; Line 1 is the fitting curve of the formal 50 frames; Line 2 is the fitting curve of the latter 50 frames.

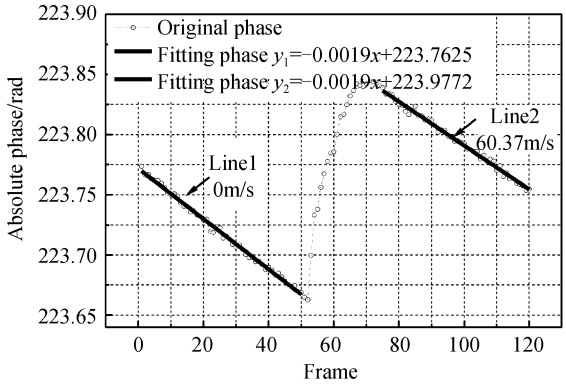

Fig.6 Time series of the average phase at L_{opt} for a single interferogram

Since the sampling time lasts for 2 min, the system drift was regarded as uniformity. Therefore the slope of the fitting curve at 0 m/s (k_1) is approximately equal to the slope of the fitting curve at 60.37 m/s (k_2). The slope difference (k_1-k_2) is 0.85 mrad that leads to a wind speed error of 0.25 m/s. It is caused by the random noise and can be negligible for this measurement.

Following the phase drift correction method above, the middle point of y_2 is (95, 223.8000) and the phase shift is 0.2146 rad. Without correction, the mean value of the phase series was regarded as the absolute phase at a given speed and the wind speed is calculated as the following Table 2

Table 2 Phase and wind retrieval before and after correction

	Phase shift/rad	Retrieved wind speed/(m·s^{-1})	Absolute wind speed/(m·s^{-1})
Before correction	0.100 6	29.59	30.78
After correction	0.214 6	63.88	3.51

Table 2 shows that the wind speed precision is improved obviously based on the method. Since the Doppler wheel can be used to simulate a wind speed in the large range, several groups of experiment under different wind speed were conducted in the laboratory.

The wind speed was simulated in the laboratory from 33.75 m/s to 75.75 m/s using the Doppler wheel, show in FIg.7. The retrieved wind speed from the change of fringe phase (round symbol curve) shows a good agreement with simulated wind. The mean error of the twelve groups of measurements is 2.97 m/s. It is shown that by correcting the drift using the linear fitting method, the wind can be retrieved with high precision.

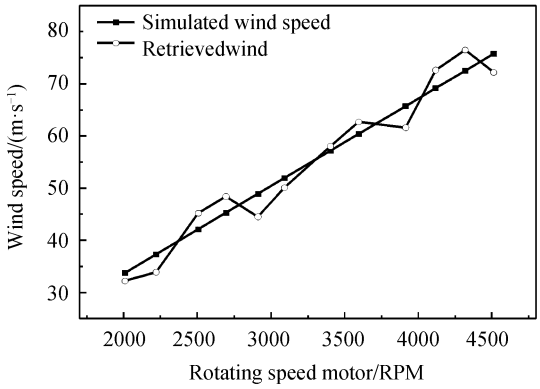

Fig.7 The retrieved wind speed

4 Discussion

It is indicated that the phase drift correction method according to a series of interferogram is suited for the experimental validation in the laboratory where only one light source is used. While in the outside detection, we can combine this method with the phase drift tracking by the calibration line together to get higher wind precision. By sampling the interferogram continuously, the phase drifts can be corrected. Therefore a loosely temperature controlling can meet the demand. However, in order to calibration the system parameters such as the Littrow wave number, a temperature controller of the interferometer with the precision of 0.1℃ is needed.

5 Conclusion

It is known that small phase error can lead to the wind retrieving error based on the Doppler Asymmetric Spatial Heterodyne (DASH) technique. We have shown in this article a new method to track and correct the phase drift without using the calibration line. By sampling the interferogram continuously at different wind speed, the phase drift which is expressed as the slope of phase curve can be recorded. It is corrected through calculating the distance from the middle point of fitting curve at a given speed to the fitting phase curve at zero wind speed. To validate the phase drift correction method, the DASH interferometer was designed and the wind detection system was established in the laboratory. The measurement was made by simulating the wind speed (60.37 m/s) with a Doppler wheel (3600 RPM).The phase drift is fitted with a slope of −0.001 9. The phase shift is 0.214 6 rad and the wind speed is retrieved with an error of 3.51 m/s. It is noted that the slope of two phase fitting curves has a difference of 0.85 mrad due to the random noise of the system. It leads to a wind speed error of 0.25 m/s and was ignored in the measurement. Using this method, several groups of measurements were conducted. The experimental measurement covered the wind speed from 33.75 m/s to 75.75 m/s and the results shows an average wind error of 2.97 m/s. It is suggested that the phase drift correction method is effective in eliminating the phase error and can be used together with a calibration lamp to get higher wind retrieving precision.

References

[1] WANG Ying-jian, WANG Yong-mei, WANG Hou-mao. Simulation of ground-based Fabry-Perot interferometer for the measurement of upper atmospheric winds[J]. *Chinese Journal of Chinese Journal of Geophys*, 2014, **57**(6): 1732-1739.

[2] ABREU V J, HAYS P B, SKINNER W R, *et al*. The high resolution Doppler imager[J]. *Optics Photon*, 1991, **2**(10): 28-30.

[3] SKINNER W R, JOHNSON R M, WU Q. TIMED Doppler interferometer (TIDI)[C]. SPIE, 1999, **3756**: 289-301.

[4] KILLEEN T L, WU Q, SOLOMON S C, *et al*. TIMED doppler interferometer: overview and recent results[J]. *Journal of Geophysical Research Space Physics*, 2006, **111**(10): 469-501.

[5] GAULT W A, JOHNSTON S F, KENDALL D J. Optimization of a field-widened Michelson interferometer[J]. *Applied Optics*, 1985, **24**(11): 1604-1608.

[6] THUILLIER G, HERSE M. Thermally stable field compensated Michelson interferometer for measurement of temperature and wind of the planetary atmospheres[J]. *Applied Optics*, 1991, **30**(10): 1210-1220.

[7] SHEPHERD G G, THUILLIER G, GAULT W A, *et al*. WINDII, the wind imaging interferometer on the upper atmosphere research satellite[J]. *Journal of Geophysical Research: Atmospheres* (1984-2012), 1993, **98**(D6): 10725-10750.

[8] SHEPHERD G G. Application of Doppler Michelson imaging to upper atmospheric wind measurement[J]. *Applied Optics*, 1996, **35**(16): 2764-2773.

[9] ENGLERT C R, HARLANDER J M, BABCOCK D D, *et al*. Doppler Asymmetric Spatial Heterodyne Spectroscopy (DASH): An innovative concept for measuring winds in planetary atmospheres[C]. SPIE Optics + Photonics. International Society for Optics and Photonics, 2006: 63030T.

[10] ENGLERT C R, HARLANDER J M, EMMERT J T, *et al*. Initial ground-based thermospheric wind measurements using Doppler asymmetric spatial heterodyne spectroscopy (DASH) [J]. *Optics Express*, 2010, **18**(26): 27416-27430.

[11] HARLANDER J M, ENGLERT C R, BABCOCK D D, *et al*. Design and laboratory tests of a Doppler Asymmetric Spatial Heterodyne (DASH) interferometer for upper atmospheric wind and temperature observations[J]. *Optics Express*, 2010, **18**(25): 26430-26440.

[12] ENGLERT C R, HARLANDER J M, BROWN C M, *et al*. Coincident thermospheric wind measurements using ground-based Doppler Asymmetric Spatial Heterodyne (DASH) and Fabry-Perot Interferometer (FPI) instruments[J]. *Journal of Atmospheric and Solar-Terrestrial Physics*, 2012, **86**(5): 92-98.

[13] XIANG Li-bin, CAI Qi-sheng, DU Shu-song. Large aperture spatial heterodyne imaging spectrometer: principle and experimental results[J]. *Optics Communications*, 2015, **357**: 148-155.

[14] ENGLERT C R, HARLANDER J M, BROWN C M, *et al*. MIGHTI: the spatial heterodyne instrument for thermospheric wind measurements on board the ICON[C]. Fourier Transform Spectroscopy (FTS), 2015:FM4A.1.

[15] ENGLERT C R, BABCOCK D D, HARLANDER J M. Doppler asymmetric spatial heterodyne spectroscopy (DASH): concept and experimental demonstration[J].*Applied Optics*, 2007, **46**(29): 7297-7307.